

Supporting Information

Pd Nanocrystals with Single-, Double-, Triple-Cavities: Facile Synthesis and Tunable Plasmonic Properties

Zhiqiang Niu,^a Yu-Rong Zhen,^b Ming Gong,^a Qing Peng,^a Peter Nordlander,^b and Yadong Li*^a

^a*Department of Chemistry, Tsinghua University, Beijing, 100084, P.R. China, and*

^b*Department of Physics and Astronomy, M.S. 61, Rice University, Houston, Texas 77005-1892, United States*

1. **Experimental Details.**
2. **Theoretical Details.**
3. **Figure S1** | HRTEM image and line-scanning profile of a hollow Pd nanoparticle.
4. **Figure S2** | TEM image of nanostructures observed in a 40-min reaction.
5. **Figure S3** | TEM images of hollow Pd nanocrystals with different cavity distributions.
6. **Figure S4** | TEM images of hollow Pd nanocrystals with different cavity sizes.
7. **Figure S5, S6** | Theoretical adsorption spectra of Pd hollow structures.
8. **Scheme 1** | Proposed formation mechanism of Pd nanoshell geometries with multiple cavities.
9. **Table S1** | Average dimensions of monomers and dimers produced with different quantities of PVP.

Experimental Details

Reagents: Palladium(II) chloride (PdCl_2 , > 59.0%), hydrochloric acid (HCl, 36%), ammonium hydroxide (NH_4OH , 25%–28%), poly (vinylpyrrolidone) (PVP, Mw: 360,000) of A.R. grade were obtained from Sinopharm Chemical Reagent Co., Ltd.

Characterization: X-ray diffraction patterns were recorded with a Rigaku D/max 2500Pc X-ray powder diffractometer with monochromatized Cu $\text{K}\alpha$ radiation ($\lambda = 1.5406 \text{ \AA}$). TEM and HRTEM images were recorded by a JEOL JEM-1200EX working at 100 kV and a FEI Tecnai G2 F20 S-Twin working at 200 kV. The adsorption spectra were obtained via a Hitachi U-3010 UV-vis spectrometer. The FTIR spectra were performed on a Nicolet 360 FTIR ESP spectrometer.

Preparation of $\text{Pd}(\text{NH}_3)_4\text{Cl}_2$: 0.8865 g PdCl_2 was dissolved in 50 mL of 0.2 M HCl. The PH value of the solution was adjusted to 7.8 by adding 0.12 M $\text{NH}_3\cdot\text{H}_2\text{O}$. The resulting colorless solution was further diluted to 250 mL with distilled water to give the 20 mM $\text{Pd}(\text{NH}_3)_4\text{Cl}_2$ aqueous stock solution.

Synthesis of Pd hollow nanoparticles: In a typical synthesis of 56 nm Pd hollow particles, 0.1 g PVP and 5 mL $\text{Pd}(\text{NH}_3)_4\text{Cl}_2$ aqueous solution (8 mM) were mixed in a 8 mL Teflon-lined stainless-steel autoclave. The autoclave was sealed and placed in a 200 °C oven for 2 hours. After the reaction, the products were purified by water-acetone mixture via centrifugation for three times and redispersed in distilled water for further characterization.

Synthesis of Pd hollow nanoparticles with different PVP quantity: 0.025 g, 0.1 g, 0.4 g PVP was mixed with 5 mL $\text{Pd}(\text{NH}_3)_4\text{Cl}_2$ aqueous solution (8 mM) respectively. The resulting homogeneous solution was placed in a 8 mL Teflon-lined stainless-steel autoclave and heated

at 200 °C for 2 hours. The products was purified by water-acetone mixture via centrifugation three times, then redispersed in distilled water for further characterization.

Synthesis of Pd hollow nanoparticles with different metal precursor concentrations: 2, 4, 8, 12, 16, 20, and 24 mM of 5 mL Pd(NH₃)₄Cl₂ aqueous solution was mixed with 0.1 g PVP respectively. The resulting homogeneous solution was placed in a 8 mL Teflon-lined stainless-steel autoclave and heated at 200 °C for 2 hours. The products was purified by water-acetone mixture via centrifugation for three times, then redispersed in distilled water for further characterization.

Theoretical Details

Spectra: The experimental spectrum for each PVP concentration was generally composed of spectra from monomers, dimers, trimers and other aggregates. For a given PVP concentration, to make a simple but reasonable theoretical simulation, we separately calculated the spectra of monomers and dimers, which account for the majority of nanoparticles synthesized even for different PVP concentrations. The final spectra of the ensemble is obtained as a weighted average of the monomer and dimer cavity spectra with the weighting data proportional to the relative abundance of the monomer and dimer cavity particles (Figure S3b).

Monomers: Despite the shape and size dispersions, the monomers can be modeled as spherical nanoshells and described using Mie theory. The dimensions of the monomers collected in experiments and their theoretical absorption spectra from Mie calculation are presented in Table S1 and Figure S5, respectively.

Dimers: The dimers were modeled as prolate spheroids with dimensions obtained from the experimental parameters shown in Table S1. The calculation of absorption spectra was performed using Lumerical (version 6.5.5), a commercial FDTD software, with a mesh size 0.5nm inside the total-field-scattered-field (TFSF) region. For the dimer cavity particles which are not spherically symmetric, we have to take into account the random orientations of

the dimer cavity axes. In simulation, there are three orthogonal orientations for dimers: first, the semi-long axis (SLA) of the dimer parallel to the incident electric polarization; second, SLA perpendicular to the incident plane (a plane expanded by electric polarization and the propagating wave-vector; third, SLA parallel to the wave-vector. Note that the third configuration easily leads to higher order modes other than dipolar modes because of retardation effects. Assuming that the orientations of dimers are evenly distributed in any differential solid angle, we simply averaged the three calculated absorption spectra for the three orthogonal orientations to account for the random orientations. The averaged absorption spectra are shown in Figure S6. It is worth noting that if only dipolar modes are excited, such averaging of spectra over orthogonal orientations would be a rigorous treatment.

Refractive Indices: The refractive indices of the PVP (core material of the nanoshells) and the solvent (water) are 1.53 and 1.33 respectively.

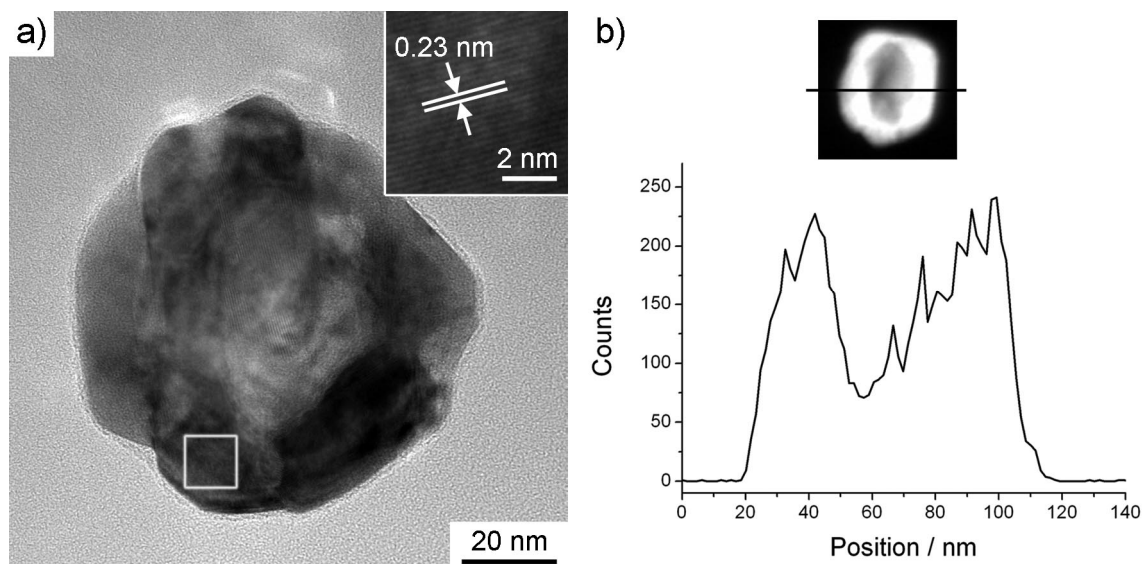


Figure S1. (a) High-resolution TEM image of hollow Pd nanoparticles. The clear lattice fringes demonstrate the good crystallinity of nanoshell. The spacing of 0.23 nm corresponds to the {111} interplanar distance of face centered cubic (fcc) Pd. (b) Line-scanning profile of one Pd nanocrystal with a single cavity.

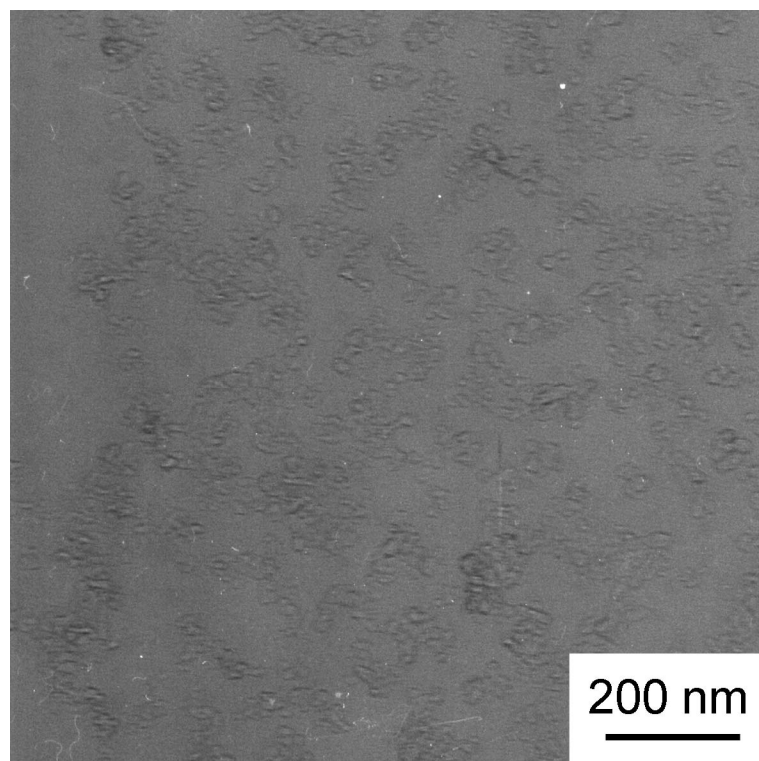


Figure S2. TEM image of nanostructures observed in a 40-min reaction.

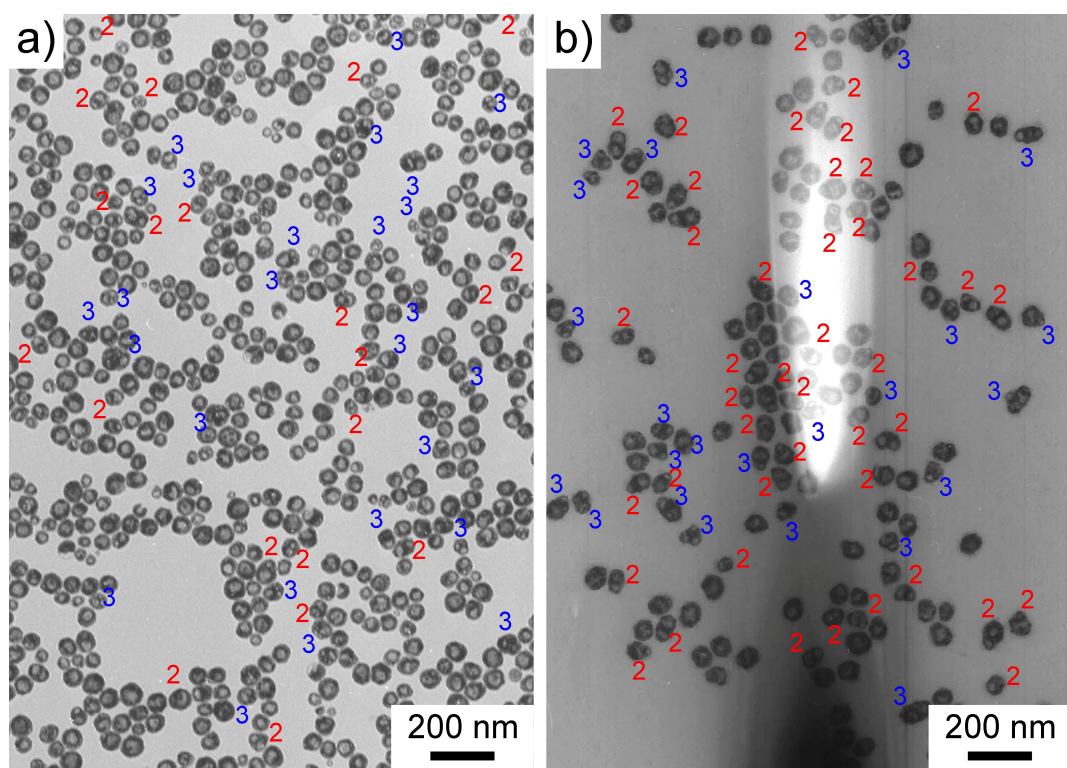


Figure S3. TEM images of hollow Pd nanoparticles prepared with (a) 0.025 g, (b) 0.4 g PVP.

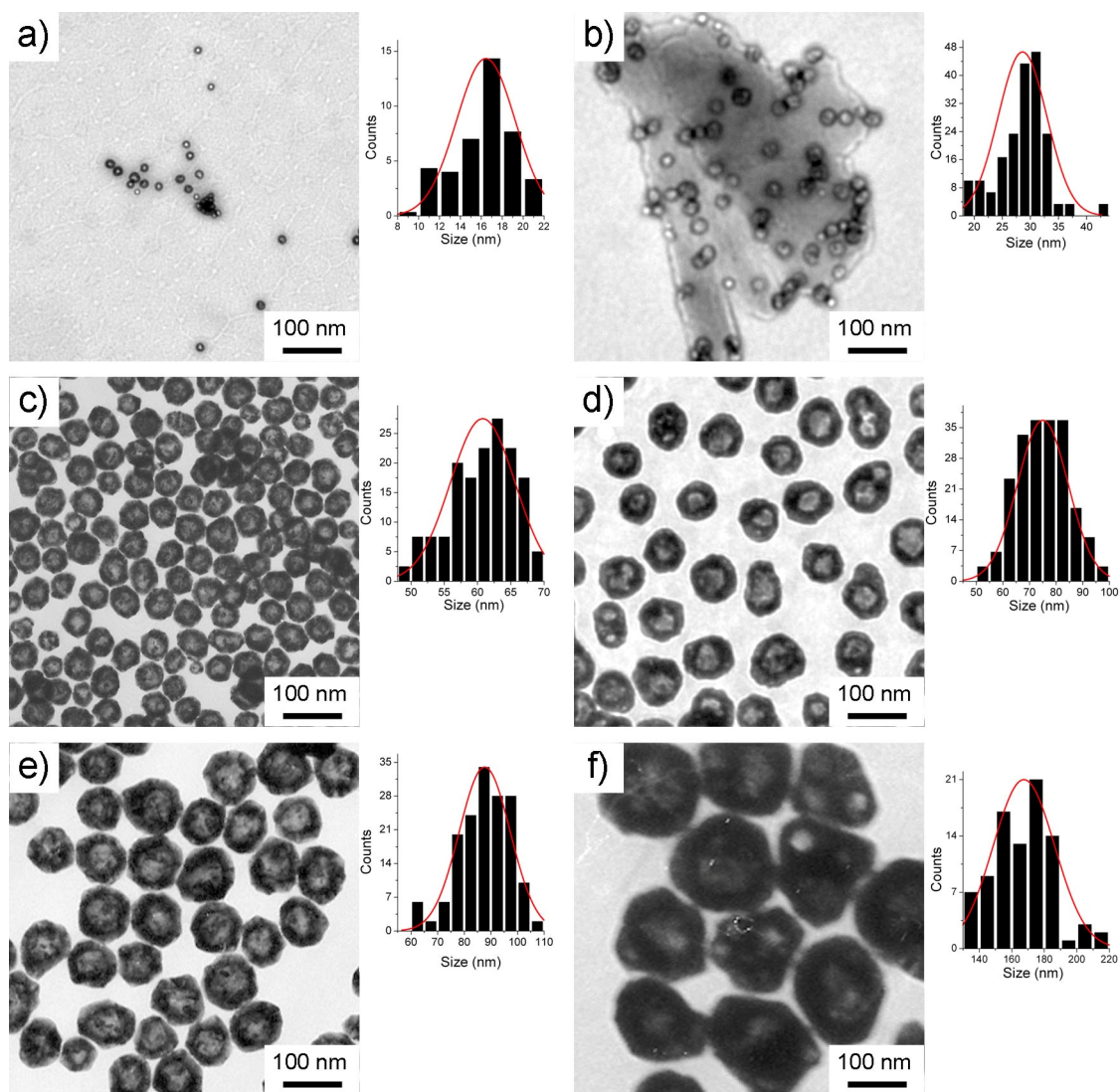


Figure S4. TEM images of hollow Pd nanoparticles synthesized by varying the metal precursor concentrations: (a) 2 mM, mean diameter: 16 nm; (b) 4 mM, mean diameter: 29 nm; (c) 12 mM, mean diameter: 61 nm; (d) 16 mM, mean diameter: 76 nm; (e) 20 mM, mean diameter: 88 nm; (f) 24 mM, mean diameter: 168 nm.

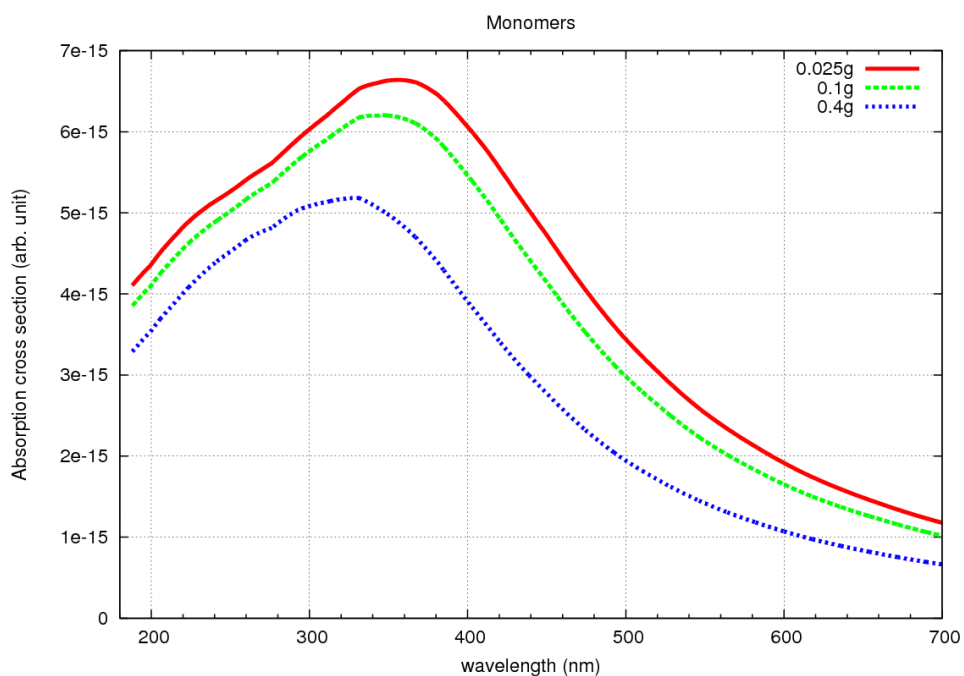


Figure S5. Absorption cross section spectra of Pd monomers (nanoshell) for 0.025g (solid), 0.1g (dash), and 0.4g (dotted). The blue-shifting of the peaks is induced by decreasing core sizes with almost unchanged shell thickness, in good agreement with plasmon hybridization⁶. Note that the intensity of resonance is also decreasing because of the diminishing cross sectional area of the nanoparticles.

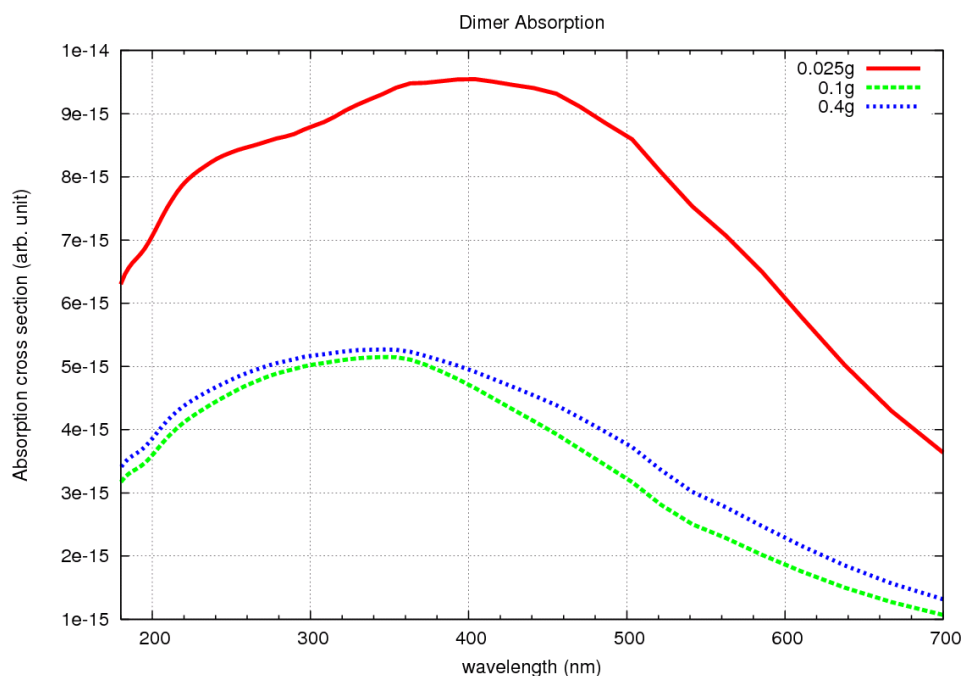
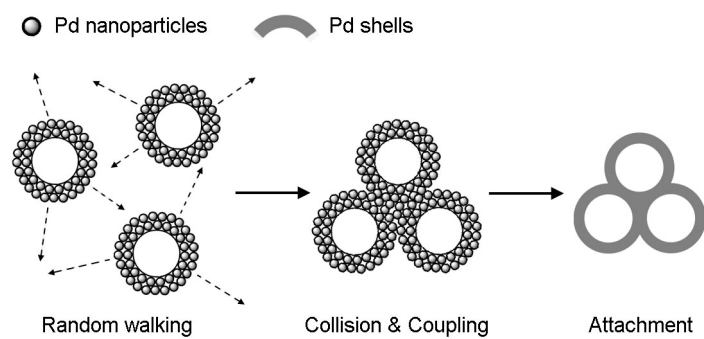


Figure S6. Orientation-averaged absorption cross section spectrum of a Pd nanoshell with a dimer cavity for 0.025g (solid), 0.1g (dash), and 0.4g (dotted).



Scheme S1. Proposed formation mechanism of Pd nanoshell geometries with multiple cavities.

Table S1. Average dimensions of monomers and dimers produced in 0.025, 0.1, and 0.4 g PVP system (8 mM metal precursor).

Sample	Monomer		Dimer (taken as ellipsoids)		
	Core radius / nm	Shell thickness / nm	Equatorial radius / nm	Polar radius / nm	Core radius / nm
0.025 g PVP	15	14	51	32	12
0.1 g PVP	14	14	36	23	9
0.4 g PVP	11	15	39	23	9